Real-Time and Full Polarimetric FM-CW Radar and its Application to the Classification of Targets

Masafumi Nakamura, Yoshio Yamaguchi, *Senior Member, IEEE,* and Hiroyoshi Yamada, *Member, IEEE*

***Abstract*—The Sinclair scattering matrix plays a decisive role in radar polarimetry. For realization of a real-time and full polarimetric radar, there are some technical problems associated with hardware implementations. Since the FM-CW radar system is suitable for short-range sensing applications, we modified an FM-CW radar to a real-time and polarimetric system by adding a PIN diode-switching circuitry for antenna polarization changes. A parallel operation scheme in the signal processing and the radar control is employed in a personal computer, which enables 44 snapshots for acquiring scattering matrices and displays the polarimetric target classification results along 44 radar ranges per second. In this paper, we present the hardware design of the system and its fundamental application to the classification of targets using the three-component decomposition theorem.**

***Index Terms*—FM-CW radar, radar polarimetry, Sinclair scattering matrix, target decomposition.**

I. Introduction

RADAR polarimetry deals with full polarimetric information of scattered waves from a target [1], [2]. It has been attracting attention in many application areas such as observation of the earth [3], [4], surveillance system for disaster, and highly advanced radar sensing [5]. The principle can be applied to any radar system whether it is pulse or CW radar [6]. The full polarimetric nature of electromagnetic wave information can be obtained by measuring a scattering matrix from a target. This scattering matrix (2×2 with complex elements) provides detailed information on the target. For example, it is possible to decompose a measured scattering matrix into a sum of three fundamental matrix components (a sphere, a diplane, and a helix) from which we can determine the dominant component and clarify the radar target. Since the principle of radar polarimetry has been established in the literature [1]–[5], the next step is to utilize the principle in the actual field. In this regard, we have been engaged in developing an FM-CW radar for short-range sensing such as subsurface applications [7], car-borne radar [8], etc.

In Section II, the design of a real-time polarimetric FM-CW radar system is described. Two transmitting and two receiving antennas are switched by a PIN-diode circuitry at several milliseconds so that quick polarization change is available. A digital signal processor (DSP) executes the fast Fourier transform (FFT) to determine a target range. The radar signal processing and operations are carried out simultaneously in the system.

In Section III, the target classification scheme using the three-component decomposition method, which has been proposed by Krogager [9], [10], is presented. This method is suitable for real-time classification of targets, because it is based on the scattering matrix information directly.

In Section IV, we present some experimental decomposition results using the explored real-time polarimetric system. Targets are plates, dihedral corner reflectors, and line targets. It is shown that the radar classifies these targets quite satisfactorily.

Manuscript received April 15, 1998; revised December 14, 1998.

The authors are with the Department of Information Engineering, Niigata University, Niigata-shi 950-2181, Japan (e-mail: yamaguch@info.eng.niigata-u.ac.jp).

Publisher Item Identifier S 0018-9456(98)09915-X.

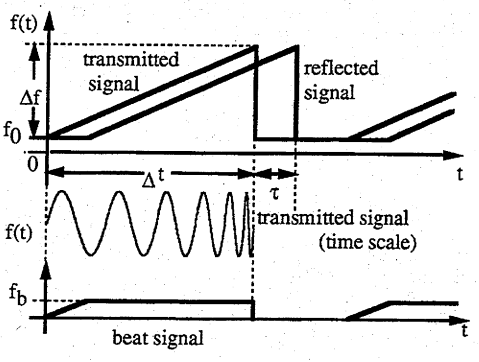

Fig. 1. Relation of frequency and time in FM-CW radar.

II. Real-Time FM-CW Radar System

An FM-CW radar transmits a linearly swept frequency signal and receives a time-delayed reflected signal from a target. Since the time delay is proportional to the beat frequency between the transmitting and receiving signals as shown in Fig. 1, the range information can be obtained by determining the frequency of the time-domain beat signal. This point benefits us in the realization of real-time radar for short-range sensing, compared to the pulse radar, because we only need to execute the Fourier transform of the time-domain beat signal once. This execution can be carried out quite quickly by using a special DSP circuit.

For polarimetric radar operation, the fundamental quantity to be measured is the Sinclair scattering matrix $[S]$, which in the linear polarization basis HV is written as

$$[S] = \begin{bmatrix} S_{HH} & S_{HV} \\ S_{VH} & S_{VV} \end{bmatrix}. \quad (1)$$

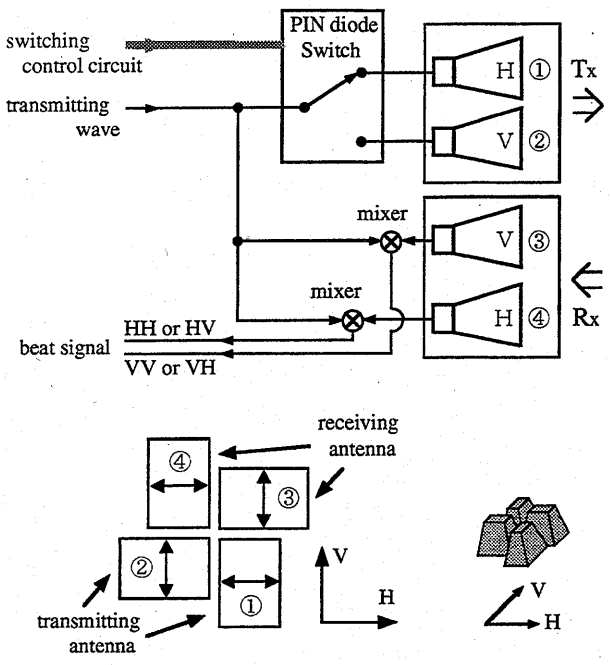

Fig. 2. Block diagram and the arrangement of antenna polarization.

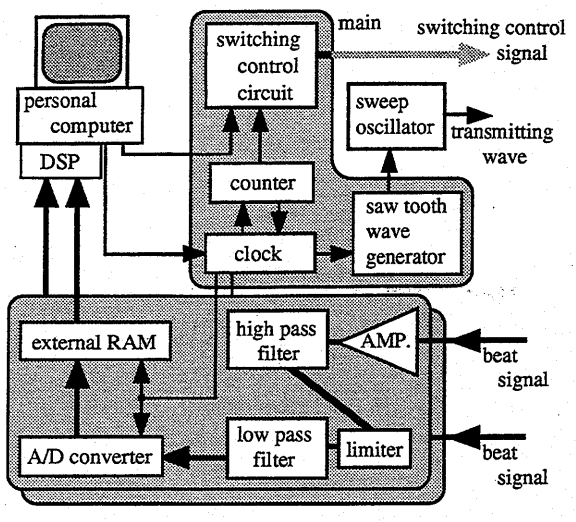

Fig. 3. Block diagram of full polarimetric FM-CW radar.

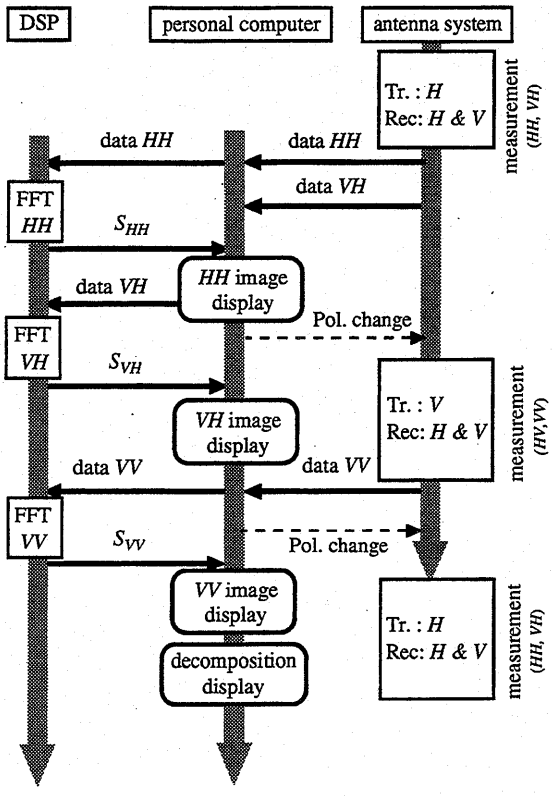

Fig. 4. Radar operational scheme.

We need to change antenna polarization quickly to acquire scattering matrix elements, i.e., S_{HH}, S_{HV}, S_{VH}, S_{VV}, where the subscript H stands for the horizontally polarized component, while the subscript V for the vertically polarized component. Assuming the radar is monostatic (which implies $S_{HV} = S_{VH}$), the minimum polarization combination required is HH, HV, and VV. Since the radar channels receive the H and V polarization components simultaneously, the only need is to switch transmitting antennas quickly. Therefore, we added a PIN diode switch at the transmitting port. Using the PIN diode switch, it is possible to change HH, HV, and VV polarization as shown in Fig. 2. Four antennas are employed in this system, two for transmission and two for receiving. It is desirable to coincide the center of four antennas at the same point for monostatic radar configuration. For example, the center for H–H and the center for V–V should be the same. However, the center for H–V locates in a different point. Since it is impossible to locate the center at the same point for all combinations, we tried to make the antenna configuration as compact as possible, avoiding antenna couplings as shown in Fig. 2.

The block diagram of the radar system is shown in Fig. 3 where the signal flow is briefly shown. A personal computer controls all of the system timing flow. It triggers a timing circuitry connected with a sweep oscillator (HP-8350B) and the switching circuit, carries out the decomposition of targets, and displays the resultant images.

The radar operation scheme is shown in Fig. 4. In this system, the personal computer, the DSP board, and the antenna system work in a cooperative manner. For example, the antennas measure simultaneously the H and V components of a target echo for the H polarized wave transmission (snapshot). The DSP receives the raw data HH of the beat signal and executes the FFT for the range signal processing. After completing the FFT in the DSP, the computer receives the resultant data set of S_{HH} and displays the HH image in the range direction. Then it sends the raw data VH to the DSP and also sends the polarization change signal to the PIN diode switch for the orthogonal polarization mode measurement. The computer then receives the next data set of S_{VH} for displaying the VH image. Again, it receives the raw data VV from the antenna system and sends it to the DSP. After a set of the scattering matrix components S_{HH}, S_{HV}, and S_{VV} is obtained, the computer carries out the decomposition of targets in the range direction. In this

way, the radar system repeats the same procedure for the next snapshot. As shown in Fig. 4, a parallel execution scheme is employed for shortening the total execution time. The control program including CRT display routine is written by assembler language so that maximum speed is attained. The total time required is 22.5 ms from a snapshot to the resultant information display. Within 22.5 ms, the radar measures approximately 104 scattering matrices along one range and displays the resultant polarimetric reflection echo with the classification results based on the decomposition (to be explained in the next section). Therefore, real-time classification operations are available in this polarimetric radar system.

Since the IF circuit is independent of microwave frequency, it is possible to change radar frequency at any band. In this case, we employed the X-band frequency (10.5–11.5 GHz).

III. Decomposition of Scattering Matrix

In the monostatic radar case, the off-diagonal elements of a scattering matrix (1) are the same ($S_{HV} = S_{VH}$). This condition implies that the scattering matrix is symmetric. If the scattering matrix is symmetric in the HV polarization basis, it is also symmetric in the circular polarization basis LR. This symmetry in the circular polarization basis is convenient to uniquely decompose an arbitrary scattering matrix into the sum of three fundamental components, i.e., a sphere, a diplane (dihedral corner reflector), and helix component matrices which represent single reflection, double reflection, and generation of circular polarization, respectively, from the radar phenomenological point of view. The three-component decomposition theorem has been proposed by Krogager [9], [10] as follows:

$$[S] = e^{j\varphi}\{e^{j\varphi_s}K_s[S]_{\text{sphere}} + K_d[S]_{\text{diplane}} + K_h[S]_{\text{helix}}\} \tag{2}$$

where the factors K_s, K_d, and K_h represent the magnitude contribution of each component. The phase φ_s in the first term is relative to the diplane's phase. For right-handed helix target inclusion, (2) has the explicit form

$$[S_{(LR)}] = e^{j\varphi}\left\{e^{j\varphi_s}K_s\begin{bmatrix}0 & 1\\ 1 & 0\end{bmatrix} + K_d\begin{bmatrix}e^{j2\theta} & 0\\ 0 & e^{-j2\theta}\end{bmatrix} + K_h\begin{bmatrix}e^{j2\theta} & 0\\ 0 & 0\end{bmatrix}\right\} \tag{3-a}$$

and for left-handed helix

$$[S_{(LR)}] = e^{j\varphi}\left\{e^{j\varphi_s}K_s\begin{bmatrix}0 & 1\\ 1 & 0\end{bmatrix} + K_d\begin{bmatrix}e^{j2\theta} & 0\\ 0 & e^{-j2\theta}\end{bmatrix} + K_h\begin{bmatrix}0 & 0\\ 0 & e^{-j2\theta}\end{bmatrix}\right\}. \tag{3-b}$$

Matching the elements of the scattering matrix for the right helix

$$[S_{(LR)}] = e^{j\varphi}\begin{bmatrix}(K_d+K_h)e^{j2\theta} & K_se^{j\varphi_s}\\ K_se^{j\varphi_s} & K_de^{-j2\theta}\end{bmatrix} = \begin{bmatrix}|S_{LL}|e^{j\varphi_{LL}} & |S_{LR}|e^{j\varphi_{LR}}\\ |S_{LR}|e^{j\varphi_{LR}} & |S_{RR}|e^{j\varphi_{RR}}\end{bmatrix} \tag{4-a}$$

TABLE I
Amplitude Factors for Elementary Targets

	K_s	K_d	K_h
sphere, plate, trihedral	1	0	0
diplane, corner reflector	0	1	0
wire	0.5	0.5	0
right / left helix	0	0	1

and for the left helix

$$[S_{(LR)}] = e^{j\varphi}\begin{bmatrix}K_de^{-j2\theta} & K_se^{j\varphi_s}\\ K_se^{j\varphi_s} & (K_d+K_h)e^{j2\theta}\end{bmatrix} = \begin{bmatrix}|S_{LL}|e^{j\varphi_{LL}} & |S_{LR}|e^{j\varphi_{LR}}\\ |S_{LR}|e^{j\varphi_{LR}} & |S_{RR}|e^{j\varphi_{RR}}\end{bmatrix} \tag{4-b}$$

yields the magnitudes K_s, K_d, and K_h in terms of the element of the scattering matrix in the circular polarization basis as

$$K_s = |S_{LR}|, \quad K_d = |S_{LL}|, \quad K_h = |S_{RR}| - |S_{LL}| \quad \text{for } |S_{RR}| > |S_{LL}| \tag{5-a}$$

$$K_s = |S_{LR}|, \quad K_d = |S_{RR}|, \quad K_h = |S_{LL}| - |S_{RR}| \quad \text{for } |S_{RR}| < |S_{LL}| \tag{5-b}$$

and the phase components as

$$\theta = \tfrac{1}{4}(\varphi_{LL} - \varphi_{RR}) \tag{6}$$

$$\varphi = \tfrac{1}{2}(\varphi_{LL} + \varphi_{RR}) \tag{7}$$

$$\varphi_s = \varphi_{LR} - \tfrac{1}{2}(\varphi_{LL} + \varphi_{RR}). \tag{8}$$

Theoretical contributions of K_s, K_d, and K_h for elementary targets are listed in Table I.

If a scattering matrix is obtained, it is possible to determine the contribution of each component by

$$\frac{K_i}{K_s + K_d + K_h} \qquad (i = s,\ d,\ h). \tag{9}$$

After examining the value, we clarify the measured scattering matrix as one of the elementary scattering matrices. In this way, it is possible to seek a best-match type and examine the scattering nature.

It is interesting to note in Table I that a wire target consists of diplane and sphere components with 50% contributions, although the physical shape is quite simple. The wire target means a straight and long line target whose radius is much smaller than the wavelength

$$[S]_{\text{wire}} = \tfrac{1}{2}([S]_{\text{diplane}} + [S]_{\text{sphere}}). \tag{10}$$

If a scattering matrix was recognized as a wire or diplane using (9), there is a possibility to determine the orientation

angle θ by (6). It should be noted that the absolute phase φ in (2) is dependent on the target range caused by the phase shift in propagation path, and that the orientation angle (6) is independent of the range. The orientation angle θ can be determined by the relative scattering matrix only. However, there exists uncertainty in the orientation angle θ such that

$$[S]_{\text{diplane}(\theta)} = \begin{bmatrix} e^{j2\theta} & 0 \\ 0 & e^{-j2\theta} \end{bmatrix}$$

$$[S]_{\text{diplane}(\theta+(\pi/2))} = \begin{bmatrix} e^{j2(\theta+(\pi/2))} & 0 \\ 0 & e^{-j2(\theta+(\pi/2))} \end{bmatrix} = -\begin{bmatrix} e^{j2\theta} & 0 \\ 0 & e^{-j2\theta} \end{bmatrix}. \quad (11)$$

This means the diplanes oriented $\theta°$ and $\theta+ 90°$ give the same form of scattering matrix in the same range except for the sign. In this case, it is necessary to take the phase φ_s (3-a) of the sphere into account. Since there exists uncertainty of $2n\pi$ $(n = 0, 1, 2, 3, \cdots)$ in the phases θ, φ, and φ_s, we can eliminate this uncertainty by putting $\varphi_s = 0$ for the wire target case. This elimination results in the determination of the orientation angle θ. In the situation that the detected target is recognized as a diplane, it is impossible to distinguish whether the orientation angle is $\theta°$ or $\theta+ 90°$. This point will be examined by an experiment which follows.

IV. Real-Time Classification Experiment

A target classification experiment was carried out in a laboratory to show the effectiveness and usefulness of the real-time and polarimetric FM-CW radar. The radar antennas are mounted on a rail 115.5 cm above an electromagnetic wave absorber surface. They were scanned along the rail in the horizontal direction to acquire scattering matrices at a constant speed. It took 7 s from the start to the end, yielding 300 snapshot results. It should be noted that the radar acts as a real aperture FM-CW radar. The beam width is approximately 18° which makes the footprint size approximately 40 × 36 cm^2. Therefore the scattering matrix obtained here is from the real aperture (low-resolution) image.

Case A—Target in the Same Range: The target arrangement is shown in Fig. 5, where the scene and the plan view are illustrated. The targets are a plate (same as sphere polarization characteristics, 25 cm each side), a straight line target (same as wire characteristics, 18 cm × 85 cm area, orientation angle = 90°), and a dihedral corner reflector (same as diplane, 20 cm each side, orientation angle = 0°). This straight line target is made of corrugated parallel plates. The measured scattering matrix in the HV polarization basis is transformed into the circular LR basis in which the target decomposition is carried out in the personal computer. The classification result in the circled area (imaging plane) shown by the dotted line in Fig. 5 is displayed on the CRT screen in real-time as shown in Fig. 6.

Fig. 6 shows the three-component classification result. The vertical axis represents the range from the radar (30.4–197.6 cm), and the horizontal axis is the scanning direction (0–180 cm) which is proportional to the scan time. The targets are

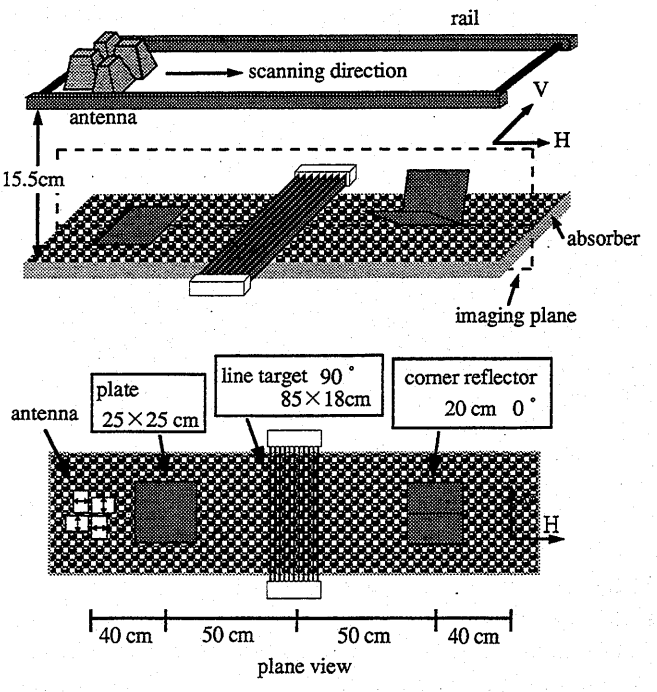

Fig. 5. Experimental scheme and target arrangement (Case A).

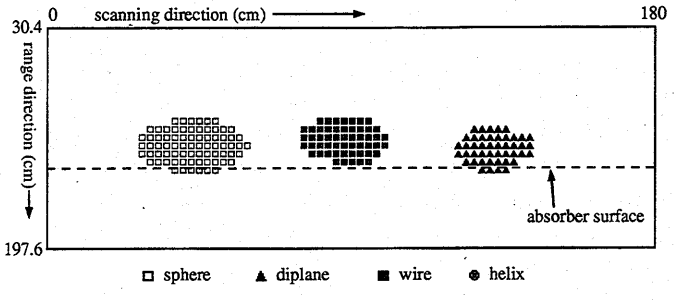

Fig. 6. Decomposition result of Case A.

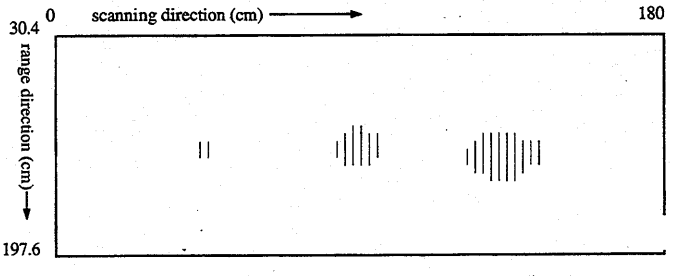

Fig. 7. Detected orientation angle of Case A.

completely classified by the radar. In addition, the orientation angle of the straight line target was found out by the scattering matrix based on (5). The detection result of the orientation angle is shown in Fig. 7 where the line indicates the direction. Since the angle is quite close to the actual orientation, it is confirmed in this case that the polarimetric system is highly useful for classification of targets and the determination of the orientation angles.

Case B—Target in a Different Range: For classification of targets in different ranges, we repeated a similar experiment

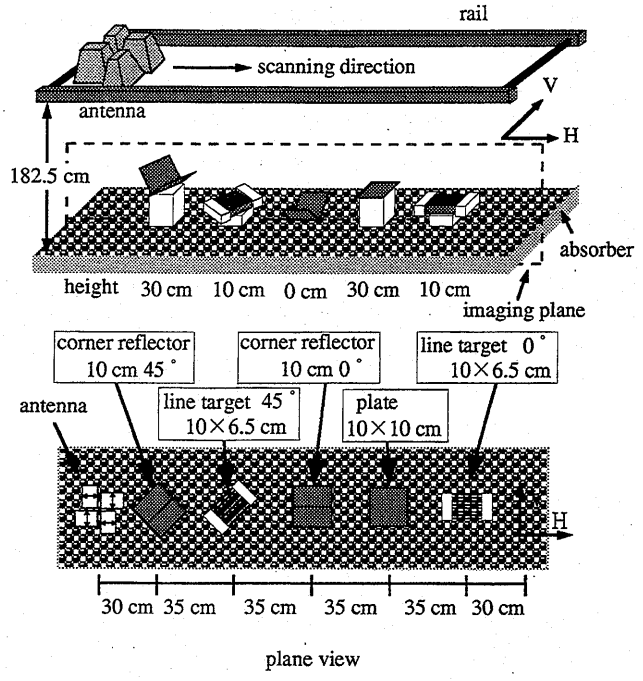

Fig. 8. Experimental scheme and target arrangement (Case B).

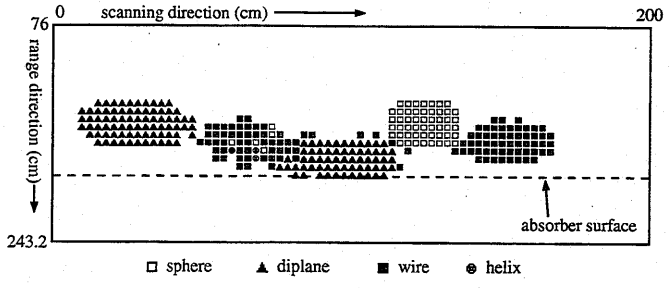

Fig. 9. Decomposition result of Case B.

as shown in Fig. 8. The targets are two straight line targets (10 cm × 6.5 cm, with orientation angles of 0 and −45°), a plate (10 cm × 10 cm), and a corner reflector (10 cm each side, 45° orientation).

Fig. 9 shows the three-component classification result of these targets. The imbalance (2:1) to (1:2) of K_d and K_s components was allowed to recognize a straight line target. Although a target whose scattering nature is similar to that of a helix was omitted in the experiment, the radar could classify these targets quite well as shown in Fig. 9. This result supports the validity of the decomposition method and the usefulness of the real-time radar system.

In addition, the detection result of the orientation angle is shown in Fig. 10. Since the diplane reflects the incident wave toward the radar in a wide range of incidence directions, the detected angle area occupies a rather wide area compared to that of the line target, due to the real aperture radar system. As mentioned in the previous section, the diplanes oriented θ and $\theta+(\pi/2)$ degrees give the same form of scattering matrix except for the sign (11). Therefore, it is difficult to distinguish the two angles by this decomposition method as pointed out in the previous section. However, the detection angle of $\theta = 45°$ is in quite good agreement with the actual orientation.

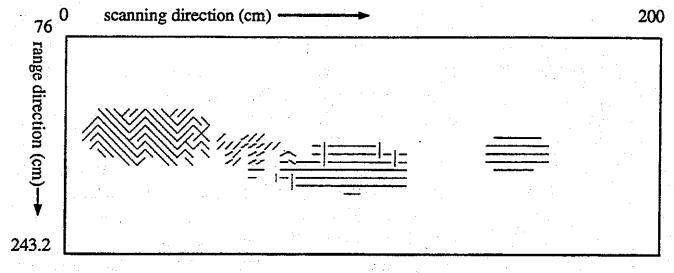

Fig. 10. Detected orientation angle of Case B.

V. Conclusion

In this paper, we demonstrated a real-time and full polarimetric FM-CW radar system. A parallel operation scheme in the signal processing and the radar control was employed in a personal computer, which enabled 44 snapshots and polarimetric target classification displays per second. A target classification experiment based on the three-component decomposition theorem was carried out to show the usefulness of the system. It is confirmed in this experiment that the radar classifies the targets quite well. This system can be used for short-range sensing applications such as car-borne radar systems.

References

[1] W.-M. Boerner, W. L. Yan, A.-Q. Xi, and Y. Yamaguchi, "On the basic principles of radar polarimetry: The target characteristic polarization state theory of Kennaugh, Huynen's polarization fork concept, and its extension to the partially polarized case," *Proc. IEEE,* vol. 79, pp. 1538–1550, Oct. 1991.

[2] H. Mott, *Antennas for Radar and Communications—A Polarimetric Approach.* New York: Wiley, 1992.

[3] F. T. Ulaby and C. Elach, *Radar Polarimetry for Geoscience Applications.* Norwood, MA: Artech House, 1990.

[4] J. A. Kong, Ed., *Polarimetric Remote Sensing, PIER3.* Amsterdam, The Netherlands: Elsevier, 1990.

[5] *Proc. 3rd Int. Workshop Radar Polarimetry,* Nantes, France, 1995.

[6] Y. Yamaguchi, T. Nishikawa, and M. Sengoku, "Fundamental study on synthetic aperture FM-CW radar polarimetry," *IEICE Trans. Commun.,* vol. E77-B, no. 1, pp. 73–80, 1994.

[7] Y. Yamaguchi and T. Moriyama, "Polarimetric detection of objects buried in snowpack by a synthetic aperture FM-CW radar," *IEEE Trans. Geosci. Remote Sensing,* vol. 34, pp. 45–51, Jan. 1996.

[8] Y. Yamaguchi, M. Sengoku, and S. Motooka, "Using a van-mounted FM-CW radar to detect corner-reflector road-boundary markers," *IEEE Trans. Instrum Measur.,* vol. 45, pp. 793–799, Aug. 1996.

[9] E. Krogager and Z. H. Czyz, "Properties of the sphere, diplane, helix decomposition," in *Proc. 3rd Int. Workshop Radar Polarimetry,* Mar. 1995, vol. 1, pp. 106–114.

[10] E. Krogager, J. Dall, and S. N. Madsen, "The sphere, diplane, helix decomposition recent results with polarimetric SAR data," in *Proc. 3rd Int. Workshop Radar Polarimetry,* Mar. 1995, vol. 2, pp. 621–625.

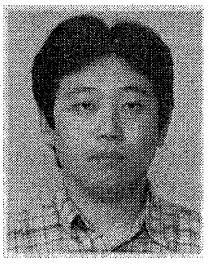

Masafumi Nakamura was born in Niigata Prefecture, Japan, on April 2, 1972. He received the B.E. degree in information engineering from Niigata University in 1996.

He is now a graduate student pursuing the M.E. degree at Niigata University, where he is engaged in SAR image analysis and target classification using radar polarimetry.

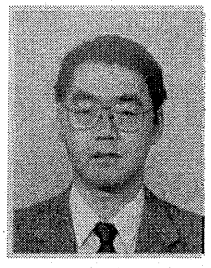

Yoshio Yamaguchi (M'83–SM'94) was born in Niigata, Japan, on March 12, 1954. He received the B.E. degree in electronics engineering from Niigata University in 1976 and the M.E. and Dr.Eng. degrees from Tokyo Institute of Technology, Tokyo, Japan, in 1978 and 1983, respectively.

In 1978, he joined the Faculty of Engineering, Niigata University, where he is a Professor. From 1988 to 1989, he was a Research Associate at the University of Illinois at Chicago. His interests are in the field of propagation characteristics of electromagnetic waves in lossy medium, radar polarimetry, and microwave remote sensing and imaging.

Dr. Yamaguchi is a member of IEICE of Japan and the Japan Society for Snow Engineering.

Hiroyoshi Yamada (M'93) was born in Hokkaido, Japan, on November 2, 1965. He received the B.S., M.S., and Ph.D. degrees from Hokkaido University, Sapporo, Japan, in 1988, 1990, and 1993, respectively, all in electronic engineering.

Since 1993, he has been with Niigata University, Niigata, Japan, where he is an Associate Professor. His current research involves superresolution techniques, time-frequency analysis, electromagnetic wave measurements, and radar signal processing.

Dr. Yamada is a member of the Institute of Electronic, Information and Communication Engineers (IEICE) of Japan.